Available online at www.sciencedirect.com
SCIENCE DIRECT®
Journal of Sound and Vibration 284 (2005) 343–360
JOURNAL OF SOUND AND VIBRATION
www.elsevier.com/locate/jsvi

The analysis of dynamic instability and vibration motions of a pinned beam with transverse magnetic fields and thermal loads

G.Y. Wu*

Department of Fire Science, Central Police University, 56 Shu-jen Rd., Ta-kang, Kwei-san, 333 Tao-yuan, Taiwan, Republic of China

Received 15 September 2003; received in revised form 10 June 2004; accepted 15 June 2004
Available online 18 November 2004

Abstract

Dynamic instability and transient vibrations of a pinned beam with transverse magnetic fields and thermal loads are studied. The magnetoelastic model, whose beam thickness and the deflection are very small compared with the length, is taken for analysis. Applying the Hamilton's principle, the equation of motion with damping factor is derived. The governing equation is reduced to the Mathieu equation by Galerkin's method with the assumed mode shape. The incremental harmonic balance (IHB) method is applied to analyze the dynamic instability. The amplitude versus time behavior of the system is investigated by using the Runge–Kutta method. The study shows that the instability and transient vibratory behaviors of the beam are influenced by the magnetic fields, thermal loads, and the frequencies of oscillation of the transverse magnetic field. The beat phenomenon and primary resonance are presented and discussed when the frequencies of the oscillating transverse magnetic field are close to the fundamental natural frequency of the system.

1. Introduction

The field of magneto elasticity has already been developing since past decades. The problems of electromagnet-mechanics on structural instability are very important in industrial applications.

*Tel.: +886 3 318 5326; fax: +886 3 328 1114.
E-mail address: una210@sun4.cpu.edu.tw (G.Y. Wu).

0022-460X/$ - see front matter © 2004 Elsevier Ltd. All rights reserved.
doi:10.1016/j.jsv.2004.06.034

One of the reviews on magnetic elasticity has been written by Ambartsumian [1]. Moon and Pao [2,3] experimentally discovered the magnetoelastic buckling and parametric instability of a cantilever beam-plate in a uniform transverse magnetic field. Through their study, a mathematical model is proposed with distributed magnetic forces and torques, which has propelled many investigations. Miya et al. [4,5] applied experimental and finite element methods to study magnetoelastic buckling on a cantilevered beam-plate. Eringen [6] derived the fields equations for elastic plates subjected to small dynamical loads and electromagnetic fields. The dynamic stability of a plate strip in a magnetic field parallel to the plan of motion is considered by Lee [7] with the destabilizing effect due to the magnetic damping. Shih et al. [8] derived the equation of motion for elastic beam under pulsating axial load and oscillating transverse magnetic field.

Recently, Tagaki et al. [9] demonstrated another phenomenon in magnetoelastic interactions, i.e., the increase of natural frequency of a ferromagnetic plate due to an increasing magnetic intensity. In order to analyze these experimental phenomenon, several theoretical models and numerical programs have been developed for studying the effect of magnetoelastic interactions upon the mechanical behavior of ferromagnetic structures [10–14]. However, thermal effect/buckling may be an undesired phenomenon for the structures because the properties of their static and dynamic characteristic would be changed. Most of the studies in the literature for vibration or instability of structures under an applied magnetic field are analyzed by considering the temperature of the structure and the conductivity of the material as a constant. The effect of variation of thermal loads on the magnetic force exerted on the structure was not considered. In reality, the magnetic force and the temperature variation have the interactive effect on the vibration and instability behavior of the structure. The means of estimation of thermal effect have to be found. The interaction between magnetic fields and a uniform temperature increment of the beam as one of the electromagnet-solid problem is a fundamental subject.

The interests of the present study are the dynamic instability and transient vibrations of a beam under magnetic fields and thermal loads. In this study, the equation of motion is derived by Hamilton's principle in which the damping parameter and induced currents are considered. Using Galerkin's method, the governing equation is reduced to a time-dependent Mathieu equation. In order to analyze the dynamic instability of this system, the incremental harmonic balance (IHB) method is adopted. The IHB method has been successfully applied to various types of linear and nonlinear structural systems [15–18]. Using the Runge–Kutta method, the transient amplitude versus time are determined from the model equation with different magnetic fields, thermal loads, and frequencies of the structure subjected to oscillating transverse magnetic field. The numerical results display some interesting characteristics on vibration of the beam having magnetic fields and thermal loads.

2. Equation of motion

In this study, an elastic beam of thickness h, width d, and length L which is pinned at its ends is considered, as shown in Fig. 1. An applied alternating uniform transverse magnetic field $B_0 = B_m \cos(\varpi t)\vec{\mathrm{j}}$ in y-direction and a uniform temperature increment ΔT are applied to the beam. The beam is initially straight having uniform thickness and the material property is assumed to be linearly elastic, isotropic and homogeneous. The cross section of the beam is

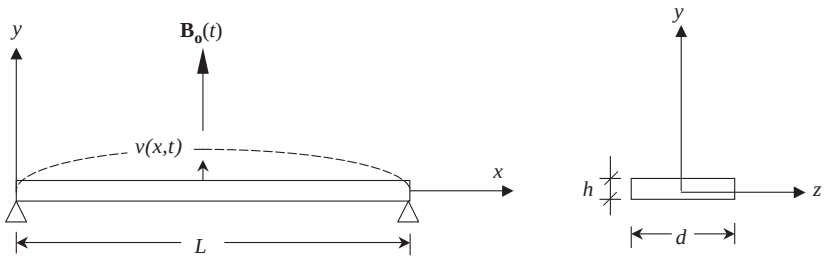

Fig. 1. The model of a beam.

symmetric. It is also assumed that the beam thickness and the deflection compared with the length are very small. As a consequence, the shear and inertia effects are neglected.

2.1. Hamilton's principle

The integral of the Langrangian function, I_L, can be written as

$$I_L = \int_{t_1}^{t_2} (K + W - U)\,\mathrm{d}t + \int_{t_1}^{t_2} W_c\,\mathrm{d}t, \tag{1}$$

where K is the kinetic energy of the system, U is the potential energy, and W is the work of externally applied force, and W_c is the work of nonconservative force. The variation of I_L leads to

$$\delta I_L = \int_{t_1}^{t_2} \delta(K + W - U)\,\mathrm{d}t + \int_{t_1}^{t_2} \delta W_c\,\mathrm{d}t = 0. \tag{2}$$

For a small deflection, the associated linear strain takes the form $\varepsilon_{xx} = \partial u/\partial x$, where u is the longitudial displacement. The elastic strain energy is expressed by the formula [19]:

$$U = \int_0^L \frac{EI}{2}\left(\frac{\partial^2 v}{\partial x^2}\right)^2 \mathrm{d}x + \int_0^L \frac{A}{2E}[E\varepsilon_{xx} - \gamma(\Delta T)]^2\ \mathrm{d}x, \tag{3}$$

where E is the Young's modulus, I the moment of inertia of the cross section, v the transversal displacement, A the cross-section area, and $\gamma(\Delta T)$ the stress–temperature coefficient. Then,

$$\begin{aligned} K &= \frac{1}{2}\int_0^L m\left(\frac{\partial v}{\partial t}\right)^2\ \mathrm{d}x, \quad W_T = \int_0^L c\frac{\partial v}{\partial x}\ \mathrm{d}x, \\ W_P &= \int_0^L N(\mathrm{d}s - \mathrm{d}x) = \frac{1}{2}\int_0^L \left(\int_0^x p\ \mathrm{d}\xi\right)\left(\frac{\partial v}{\partial x}\right)^2\ \mathrm{d}x, \\ \delta W_c &= \int_0^L c_d\left(\frac{\partial v}{\partial t}\right)\delta v\,\mathrm{d}x \quad \text{and} \quad W = W_T + W_P, \end{aligned} \tag{4}$$

where m and c are the mass and the body couple of the beam per unit length, respectively. N is the axial compressive force of the beam, p is the body force of the beam per unit length, and c_d is the

damping constant. Eq. (2) can be written as

$$\begin{aligned}\delta I_L = & \int_{t_1}^{t_2}\int_0^L \left\{ m\frac{\partial^2 v}{\partial t^2} + \frac{\partial c}{\partial x} + \frac{\partial}{\partial x}\left[\left(\int_0^x p\ \mathrm{d}\xi\right)\frac{\partial v}{\partial x}\right] + EI\frac{\partial^4 v}{\partial x^4} \right. \\ & - EA\frac{\partial}{\partial x}\left\{\left[\frac{\partial u}{\partial x} - \frac{\gamma(\Delta T)}{E}\right]\frac{\partial v}{\partial x}\right\} + c_d\frac{\partial v}{\partial t}\Big\}\delta v\,\mathrm{d}x\,\mathrm{d}t \\ & + \int_{t_1}^{t_2}\left\{ EI\frac{\partial^2 v}{\partial x^2}\frac{\partial}{\partial x}(\delta v) - EI\frac{\partial^3 v}{\partial x^3}\delta v - c\delta v - \left(\int_0^x p\ \mathrm{d}\xi\right)\frac{\partial v}{\partial x}\delta v \right. \\ & \left. + EA\left[\frac{\partial u}{\partial x} - \frac{\gamma(\Delta T)}{E}\right]\frac{\partial v}{\partial x}\delta\right\}\Big|_0^L \mathrm{d}t - \int_{t_1}^{t_2}\int_0^L EA\frac{\partial}{\partial x}\left[\frac{\partial u}{\partial x} - \frac{\gamma(\Delta T)}{E}\right]\delta u\,\mathrm{d}x\,\mathrm{d}t \\ & + \int_{t_1}^{t_2} EA\left[\frac{\partial u}{\partial x} - \frac{\gamma(\Delta T)}{E}\right]\delta u\Big|_0^L \mathrm{d}t - \int_0^L \left(m\frac{\partial v}{\partial t}\delta v\right)\Big|_{t_1}^{t_2}\mathrm{d}x = 0. \end{aligned} \tag{5}$$

Assuming pinned support conditions with no horizontal and vertical displacement at $x = 0$ and L, the associated boundary conditions can be defined as

$$\begin{aligned} & \delta u(0) = \delta u(L) = \delta v(0) = \delta v(L) = 0, \\ & v(0) = v(L) = 0 \quad \text{and} \quad v''(0) = v''(L) = 0. \end{aligned} \tag{6}$$

The equilibrium equations of motion with the associated boundary conditions can be obtained as

$$EA\frac{\partial}{\partial x}\left[\frac{\partial u}{\partial x} - \frac{\gamma(\Delta T)}{E}\right] = 0, \tag{7}$$

$$m\frac{\partial^2 v}{\partial t^2} + c_d\frac{\partial v}{\partial t} + EI\frac{\partial^4 v}{\partial x^4} + \frac{\partial c}{\partial x} + \frac{\partial}{\partial x}\left[\left(\int_0^x p\ \mathrm{d}\xi\right)\frac{\partial v}{\partial x}\right] - EA\frac{\partial}{\partial x}\left\{\left[\frac{\partial u}{\partial x} - \frac{\gamma(\Delta T)}{E}\right]\frac{\partial v}{\partial x}\right\} = 0. \tag{8}$$

Eq. (7) will be satisfied with the assumption

$$\frac{\partial u}{\partial x} - \frac{\gamma(\Delta T)}{E} = \text{constant} = \bar{\delta}(\Delta T), \tag{9}$$

where $\bar{\delta}(\Delta T)$ is equal to the average strain of the system, therefore

$$\bar{\delta}(\Delta T) = \frac{1}{L}\int_0^L \left[\frac{\partial u}{\partial x} - \frac{\gamma(\Delta T)}{E}\right]\mathrm{d}x = -\frac{\gamma(\Delta T)}{E}. \tag{10}$$

Substituting Eq. (10) into Eq. (8), the equation of motion is obtained

$$m\frac{\partial^2 v}{\partial t^2} + c_d\frac{\partial v}{\partial t} + EI\frac{\partial^4 v}{\partial x^4} + \frac{\partial c}{\partial x} + \frac{\partial}{\partial x}\left[\left(\int_0^x p\ \mathrm{d}\xi\right)\frac{\partial v}{\partial x}\right] + A\gamma(\Delta T)\frac{\partial^2 v}{\partial x^2} = 0. \tag{11}$$

2.2. Electromagnetic force **F** and torque **c**

The electromagnetic force **F** and torque **c** acting on a volume V as shown by King and Prasad [20] are

$$\mathbf{F} = \int [\sigma(\mathbf{E_e} + \dot{\mathbf{r}} \times \mathbf{B_0}) \times \mathbf{B_0} + (\mathbf{M} \cdot \nabla)\mathbf{B_0}]\, \mathrm{d}V, \tag{12a}$$

$$\mathbf{c} = \int (\mathbf{r} \times \mathrm{d}\mathbf{F} + \mathbf{M} \times \mathbf{B_0})\, \mathrm{d}V, \tag{12b}$$

where $\mathbf{E_e}$ and $\mathbf{B_0}$ are the induced electric field and the magnetic field, σ is the conductivity of the material, $\mathbf{r}$ is the vector from an arbitary origin to the element $\mathrm{d}V$, $\dot{\mathbf{r}}$ is the velocity of body motion, and $\mathbf{M}$ is the volume density of magnetization in the body. The first term in $\mathbf{c}$ is known as body torque and the second term in $\mathbf{c}$ is the torque on a magnetic dipole in a uniform field. In this study, $\mathbf{B_0}$ is considered as a uniform field, therfore, $(\mathbf{M} \cdot \nabla)\mathbf{B_0} = 0$. It has been shown by Shih et al. [8] that $\int_v \sigma \mathbf{E_e} \times \mathbf{B_0}\, \mathrm{d}V = 0$ and $\int_v (\mathbf{r} \times \mathrm{d}\mathbf{F})\, \mathrm{d}V = 0$ because of the symmetric. Eqs. (12a) and (12b) can be simliplied as

$$\mathbf{F} = \int \sigma(\dot{\mathbf{r}} \times \mathbf{B_0}) \times \mathbf{B_0}\, \mathrm{d}V, \tag{13}$$

$$\mathbf{c} = \int \mathbf{M} \times \mathbf{B_0}\, \mathrm{d}V, \tag{14}$$

where $\mathbf{M} = \chi(\mu_0\mu_r)^{-1}\mathbf{B}$, $\chi = 1 - \mu_r$ is the susceptibility, μ_0 is the permeability of the vacuum, μ_r is the relative permeability, and $\mathbf{B}$ is the magnetic induction vector.

3. Analytical procedure

3.1. Displacement function

For the pinned beam, the displacement function can be written as

$$v(x,t) = \sum_{n=1,2,\ldots} w_n(t) \sin\, \lambda_n x, \quad 0 \leqslant x \leqslant L, \tag{15}$$

where $\lambda_1 = \pi/L$ for the first mode.

An inextensible beam is assumed, therefore

$$\int_0^x \left[1 + v'^2(\xi,t)\right]^{1/2} \mathrm{d}\xi = s, \tag{16}$$

where s is the length of the beam from 0 to x. Differentiating Eq. (16) with respect to t becomes

$$\int_0^x \left[\frac{v'\dot{v}'}{(1+v'^2)^{1/2}}\right] \mathrm{d}\xi + [1+v'^2]^{1/2}\dot{x} = 0. \tag{17}$$

For a small deflection $[1+v'^2]^{1/2} \approx 1$; then substituting this into Eq. (13), the velocity in x-direction can be derived as

$$\dot{x} = \dot{r}(x,w) = -\int_0^x v\dot{v}'\,\mathrm{d}\xi = \sum_{n=1,2,\ldots} -\left(\frac{\lambda_n^2}{2}\right) w_n \dot{w}_n \left[x + \left(\frac{\lambda_n}{2}\right)\sin 2\lambda_n x\right], \tag{18}$$

$$\mathbf{F} = p\vec{i} = \sum_{n=1,2,\ldots} \left(\frac{\sigma}{4}\right)\lambda_n^2 h\ dB_m^2 \left[x + \left(\frac{\lambda_n}{2}\right)\sin\ 2\lambda_n x\right](1+\cos\ 2\varpi t)\ w_n \dot{w}_n\,\vec{i}. \tag{19}$$

The magetization $\mathbf{M}$ can be derived using the same way as presented in Ref. [3], then the body couple can be obtained as

$$\mathbf{c} = \int \mathbf{M} \times \mathbf{B_0}\,\mathrm{d}V = \sum_{n=1,2,\ldots} \lambda_n \Phi_n d\cos\ \lambda_n x(1+\cos\ 2\varpi t) w_n \vec{k}, \tag{20}$$

where $\Phi_n = \chi^2 B_m^2\ \ \sinh(\lambda_n h/2)/(\mu_0 \mu_r \lambda_n \Delta_n)$ and $\Delta_n = \mu_r \sinh(\lambda_n h/2) + \cosh(\lambda_n h/2)$.

Substituting Eqs. (18–20) into Eq. (11) leads to a linear operator $\Pi(w)$:

$$\begin{aligned}\Pi(w) = \sum_{n=1,2\ldots} \Bigg\{ &\left[m\ddot{w}_n + c_d \dot{w}_n - \lambda_n^2 \Phi_n d(1+\cos\ 2\varpi t) w_n + EI\lambda_n^4 w_n - A\lambda_n^2 \gamma(\Delta T) w_n\right] \sin\ \lambda_n x \\ &- \left(\frac{\sigma}{4}\right)\lambda_n^3 h d B_m^2 (1+\cos\ 2\varpi t) w_n^2 \dot{w}_n \times \left\{ \lambda_n \left[\frac{x^2}{2} + \frac{1}{4\lambda_n^2}(1-2\cos\ 2\lambda_n x)\right] \sin\ \lambda_n x \right. \\ &\left. - \left(x + \frac{1}{2\lambda_n}\sin\ 2\lambda_n x\right)\cos\ \lambda_n x \right\} \Bigg\} = 0. \end{aligned} \tag{21}$$

3.2. Temperature effects

The conductivity σ of a material is simply reciprocal of its resistivity, so $\sigma = 1/\vartheta$, where ϑ is the resistivity of the material. The relation between the increased temperature ΔT and resistivity is considered as

$$\vartheta = \vartheta_0 + \vartheta_0 \alpha_r \Delta T, \tag{22}$$

where ϑ_0 is the resistivity and α_r the temperature coefficient of resistivity.

In this study, the linear elastic stress–temperature coefficient is defined as $\gamma(\Delta T) = EA\,\alpha\Delta T$, where α is the coefficient of thermal expansion. The thermal expansion is cancelled out by equal and opposite contraction caused by the restraining force P_t. This is because in this case the total strain is zero (no displacement) for both ends. Therefore, the magnitude of the restraining force is

$$P_t = -EA\alpha\Delta T \tag{23}$$

If the beam is slender, then it will buckle before the material reaches its yield stress. The critical load of a compressed ideal beam/column is affected by the boundary conditions. A low-carbon steel is considered, and Young's modulus $E = 1.94 \times 10^{11}$ Pa, density $\rho = 7930\,\mathrm{kg/m^3}$, length

$L = 0.4\,\text{m}$, width $d = 2.0 \times 10^{-2}\,\text{m}$, and $L/h = 100$ are chosen in this study. The critical load $P_{\text{cr}} = \pi^2 EI/l^2$ given by the Euler bulking formula is used for the first mode. Thus, the critical load P_{cr} is 1276.5 N and the critical stress σ_{cr} is 15.956 Mpa. The value of the critical stress is less than the yield stress of the material. Equating the Euler bulking formula to the restraining force P_t, the critical buckling temperature becomes

$$\Delta T_{\text{cr}} = \frac{\pi^2}{\alpha}\left(\frac{r_r}{l}\right)^2 = \frac{\pi^2}{\alpha \hbar^2}, \tag{24}$$

where r_r is the radius of gyration and $\hbar$ is the slenderness (l/r_r). This result clearly shows that the amount of restraint required is not large for slender sections to reach the buckling temperature.

3.3. Galerkin's method

The first mode ($n = 1$) is considered in this study, which means $\lambda = \pi/L$. Taking $\sin \lambda x$ as the base function, Galerkin's equation leads to

$$\int_0^L \Pi(w) \sin\ \lambda x \, \mathrm{d}x = 0. \tag{25}$$

By simplifying Eq. (25), a time-dependent differential equation is derived as follows:

$$\frac{\mathrm{d}^2 w}{\mathrm{d}t^2} + 2[\kappa + \varsigma(1 + \cos 2\varpi t)w^2]\frac{\mathrm{d}w}{\mathrm{d}t} + (\omega_L^2 - \xi \cos\ 2\varpi t)w = 0, \tag{26}$$

where ρ is the density of the beam,

$$2\kappa = \frac{c_d}{\rho h d},\ \ 2\varsigma = 2\sigma B_m^2 \lambda^2 \left(\frac{-8\lambda^2 L^2 - 18}{192\rho}\right),\ \ \omega_L^2 = \omega_0^2\left(1 - \frac{B_r^2}{B_c^2} - \frac{EA\alpha\Delta T}{P_{\text{cr}}}\right),$$

$$\omega_0^2 = \frac{EI\lambda^4}{\rho h d},\ \ B_r^2 = \frac{B_m^2}{2},\ \ B_c^2 = \frac{EI\lambda^3 \mu_0 \mu_r \Delta}{2\chi^2 d\ \sinh(\lambda h/2)},\ \ P_{\text{cr}} = EI\lambda^2 = EI\frac{\pi^2}{L^2},$$

$$\xi = \frac{\Phi\lambda^2}{\rho h}\ \ \text{and}\ \ \sigma = \frac{1}{\vartheta_0 + \vartheta_0 \alpha_r \Delta T}.$$

One recognizes ω_0 as the natural frequency of the pinned beam in a zero load, ω_L as the fundamental natural frequency of the system, and B_c as the buckling field of the system for the first mode. Since the beam is most likely to be considered at the first region of instability, the following set of variables is used [15,16]: the reduced vibration natural frequency $\Omega = \varpi/\omega_L$, a new time scale $\tau = \varpi t$, the reduced linear viscous damping $k_1 = \kappa/\omega_L$, the nonlinear damping coefficient $k_2 = \varsigma/\omega_L$, and the new coefficient of excitation $2\varphi = \xi/\omega_L^2$. Eq. (26) becomes

$$\Omega^2 \frac{\mathrm{d}^2 w}{\mathrm{d}\tau^2} + 2\Omega[k_1 + k_2(1 + \cos\ 2\tau)w^2]\frac{\mathrm{d}w}{\mathrm{d}\tau} + (1 - 2\varphi\ \cos\ 2\tau)w = 0. \tag{27}$$

3.4. Incremental harmonic balance (IHB) method and linearized equation

The IHB procedure has been provided by Lau and Cheung [15], Lau, et al. Wu [16] and Pierre and Dowell [17]. The first step is a Newton–Raphson procedure. The current state of vibration corresponding to a point (Ω_0, φ_0)on instability boundary is denoted by w_0. A neighboring state is reached through a parameter incrementation:

$$\varphi = \varphi_0 + \Delta\varphi, \quad \Omega = \Omega_0 + \Delta\Omega, \quad w = w_0 + \Delta w. \tag{28}$$

Substituting Eq. (28) into Eq. (27) and neglecting the nonlinear terms of $\Delta\varphi$, $\Delta\Omega$, Δw, a linearized incremental equation is obtained:

$$\begin{aligned}\Omega_0^2\Delta\ddot{w} + 2\Omega_0\left[k_1 + k_2(1+\cos 2\tau)w_0^2\right]\Delta\dot{w} + \left(1 - 2\varphi_0\cos 2\tau\right)\Delta w \\ + 4\Omega_0 k_2(1+\cos 2\tau)w_0\Delta w\Delta\dot{w} \\ = R + 2\Delta\varphi w_0\cos 2\tau - 2\Delta\Omega\Omega_0\ddot{w}_0 - 2\Delta\Omega\left[k_1 + k_2(1+\cos 2\tau)w_0^2\right]\dot{w}_0,\end{aligned} \tag{29a}$$

$$R = -\left\{\Omega_0^2\ddot{w}_0 + 2\Omega_0\left[k_1 + k_2(1+\cos 2\tau)w_0^2\right]\dot{w}_0 + \left(1 - 2\varphi_0\cos 2\tau\right)w_0\right\}. \tag{29b}$$

The second step is to find an approximate solution by assuming a periodic solution and applying Galerkin's method. The approximate functions w_0 and Δw can be assumed as

$$w_0(\tau) = \sum_{k=1,3,\ldots}^{2N-1}(a_k\sin k\tau + b_k\cos k\tau) \text{ and } \Delta w(\tau) = \sum_{k=1,3,\ldots}^{2N-1}(\Delta a_k\sin k\tau + \Delta b_k\cos k\tau) \tag{30}$$

for the principal region of instability corresponding to a solution of period 2π. N is the number of temporal terms for calculation. First three harmonic terms give results of high accuracy in the study of Lau et al. [16].

Substituting Eq. (30) into Eq. (29a) and using Galerkin's procedure, a set of linear equations can be obtained as follows:

$$[C]\{\Delta a\} = \{R\} + \Delta\varphi\{P\} + \Delta\Omega\{Q\}, \tag{31}$$

where $[C]$ is the matrix for the Fourier coefficients and $\{\Delta a\}$ is a vector consisting of Fourier coefficients Δa_k or Δb_k, $\{R\}$ is the corrective vector derived from Eq. (29b), and $\{P\}$ and $\{Q\}$ are vectors obtained from the second and third right-hand side terms, respectively.

From Eq. (31), a linear system of $2N$ equations with $2N+2$ unknowns Δa, $\Delta\varphi$, and $\Delta\Omega$ has to be solved at each incremental step. Hence, it is necessary to add two constraints among Δa, $\Delta\varphi$, and $\Delta\Omega$. The first constraint is $\Delta a_1 = 0$ and the second constraint either $\Delta\varphi = 0$ or $\Delta\Omega = 0$. In the study, $\Delta\varphi = 0$ has been used as the second constraint, then $\Delta\Omega$ is obtained by linear algebra method.

4. Numerical results and discussions

Numerical simulations are performed for the dynamic instability and transient vibrations of a pinned beam with transverse magnetic fields and thermal loads. The physical parameters of this

system are given as

$\mu_r = 3.0 \times 10^3\ \mathrm{Hm}^{-1}$, $\alpha = 11 \times 10^{-6}\ ^\circ\mathrm{C}^{-1}$, $\alpha_r = 6.5 \times 10^{-3}\ ^\circ\mathrm{C}^{-1}$, $\mu_0 = 1.26 \times 10^{-6}\ \mathrm{Hm}^{-1}$, $\vartheta_0 = 9.68 \times 10^{-8}\ \Omega$m(ohm-meter).

4.1. The region of dynamic instability

Considering the beam thickness and deflection to be small compared to their length, the equation of motion of a simply supported beam-plate in an alternating magnetic field without damping had been derived by Moon and Pao [3] and is written as

$$\frac{\mathrm{d}^2 w}{\mathrm{d}t^2} + \omega_L^2(1 - 2\eta\ \cos\ 2\varpi t)w = 0, \tag{32}$$

where $\omega_L^2 = \omega_0^2(1 - B_r^2/B_c^2) = \omega_0^2(1 - \bar{B}^2)$, $2\eta = B_m^2/(2B_c^2 - B_m^2) = \bar{B}^2/(1 - \bar{B}^2)$, $\bar{B}^2 = B_m^2/2B_c^2 = B_r^2/B_c^2$, and ω_0^2 is defined the same as in Eq. (26). As mentioned in Ref. [3], it is customary to discuss these solutions on the (ϖ/ω_L) versus η or the $(\varpi/\omega_0)^2$ versus $(B_r/B_c)^2$ plane and divide it into regions of stability and instability. In order to evculate the accuracy of the analytical process in this study, the parameter transformation is used to build the region of instability on the $(\varpi/\omega_0)^2$ versus $(B_r/B_c)^2$ plane by replacing the derivative parameters Ω and φ of the IHB method. The results of instability in this study and the results studied in Ref. [3] are shown in Fig. 2. These results are found to be in good agreement. Therefore, the equation of motion and the analytical method considered in this study are reasonable.

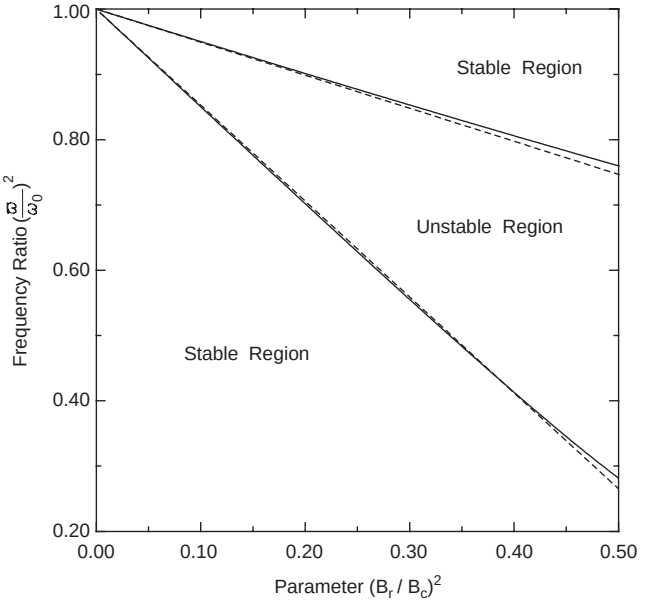

Fig. 2. The theoretical region of instability of a simply supported beam-plate in a transverse magnetic field. ---, Ref. [3]; —, present results.

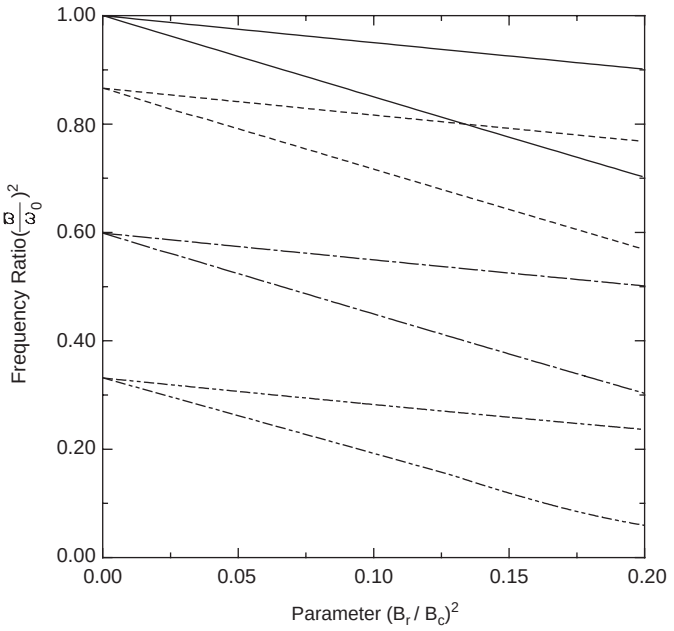

Fig. 3. The influence of thermal load on the principal region of instability in a transverse magnetic field. —, $\Delta T = 0$ °C; - - -, $\Delta T = 1.0$ °C; — - —, $\Delta T = 3.0$ °C; — - - —, $\Delta T = 5.0$ °C.

In this study, the main parameters that determine the responses of instability of the system are the uniform increased temperature, magnetic filed, and damping ratio. As derived earlier for the later thermal restraint, the critical buckling temperature is very easily achieved for slender sections in structures. In this case, the critical buckling temperature of the first mode is $\Delta T_{\rm cr} = 7.47$ °C. Now, one considers damping parameter $k_1 = 0$, then the different increased temperatures ΔT are applied. The effect of increased temperature ΔT is shown in Fig. 3, where the principal region of instability is shifted down, with increasing temperature from 0 to 5 °C, while $(B_r^2/B_c^2) + (EA\alpha\Delta T/P_{\rm cr}) < 1$. The variation of temperature can produce a large variety of responses.

Considering the different damping parameters k_1 with $\Delta T = 0$, the regions of instability are shown in Fig. 4. It shows that the region of instability decreases with increasing damping parameter k_1. In this study, it may be noted that the nonlinear damping coefficient ς is proportional to the square of amplitude, and the actual nonlinear damping constant of the system can be easily obtained from Eq. (26). For instance, under the small deflection assumption, $w/h = 1.0$, $\Delta T = 1.0$ °C, and $B_m = 0.2$ T are applied. The fundamental natural frequency ω_L is 315.95 rad/s and the magnitude of the nonlinear damping constant is 0.052 kg/s, so that the nonlinear dimensionless damping parameter k_2 now is 8.17×10^{-5}. Therefore, the effect of nonlinear damping on the region of instability is insignificant in this study. The choice of linear viscous damping parameter k_1 will be discussed in the next section.

4.2. The part of vibration

To determine the relationship between amplitude and time for the system with viscous damping, the fourth-order Runge–Kutta method is applied to solve Eq. (26) with initial

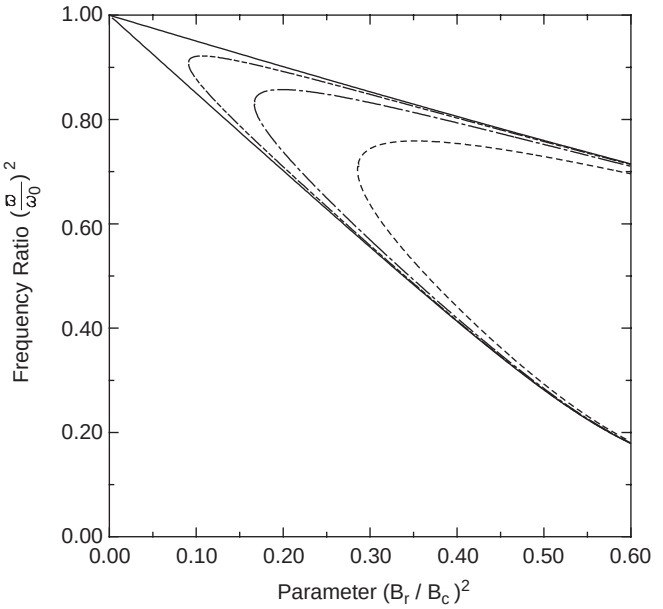

Fig. 4. The influence of damping on the principal region of instability in a transverse magnetic field. —, $k_1 = 0$; — - - —, $k_1 = 0.025$; — - —, $k_1 = 0.05$; - - -, $k_1 = 0.1$.

conditions. The step size is 2.0×10^{-5}. Initial conditions are chosen as $w_{,t} = 0$ and $w/h = 1.0$ at $t = 0$.

While the different magnetic fields $B_m = 0.1$, 0.3, 0.5 T and $\varpi = 80$ rad/s are applied with $k_1 = 0$, the results of amplitude versus time are shown in Figs. 5(a)–(c). While $B_m = 0.2$ T, $\varpi = 80$ rad/s, $k_1 = 0$, and the different increased temperatures $\Delta T = 1.0$, 3.0, 5.0 °C are applied, the results with the magnetic field and the increased temperature are shown in Figs. 6(a)–(c), respectively. It can be seen from the waveforms presented that increasing the magnetic field or/and temperature decreases the fundamental frequency of the system significantly. Therefore, the period of vibration with the magnetic field or temperature increment is increased compared with the system without the magnetic field or temperature increment. The changes of the fundamental natural frequency ω_L due to a magnetic field increment and the temperature increment ΔT as determined by solving Eq. (26) is shown. It is noted that the magnetic field increment increases the damping effect which is related to the square of the amplitude. Also, the damping effect can be related to the conductivity of the material as $\sigma = 1/(\vartheta_0 + \vartheta_0 \alpha_r \Delta T)$.

The above cases are not considered as the dynamic instability, while damping parameters $k_1 = 0.0$, $\Delta T = 3.0$ °C, and $B_m = 0.2$ T are applied. Based on Eq. (26), the fundamental natural frequency of the system becomes 258.2 rad/s. According to the analysis of the dynamic instability, the primary region of the dynamic instability occurs such that the ratio of excitation frequency with respect to the natural frequency of the system closes to 1.0, when ϖ is applied by 250.5, 258.2, and 266.5 rad/s, individually; the results of the amplitude versus time are shown in Fig. 7. From these waveforms, the beat phenomenon occurs in Figs. 7(a) and (c), and the resonance case

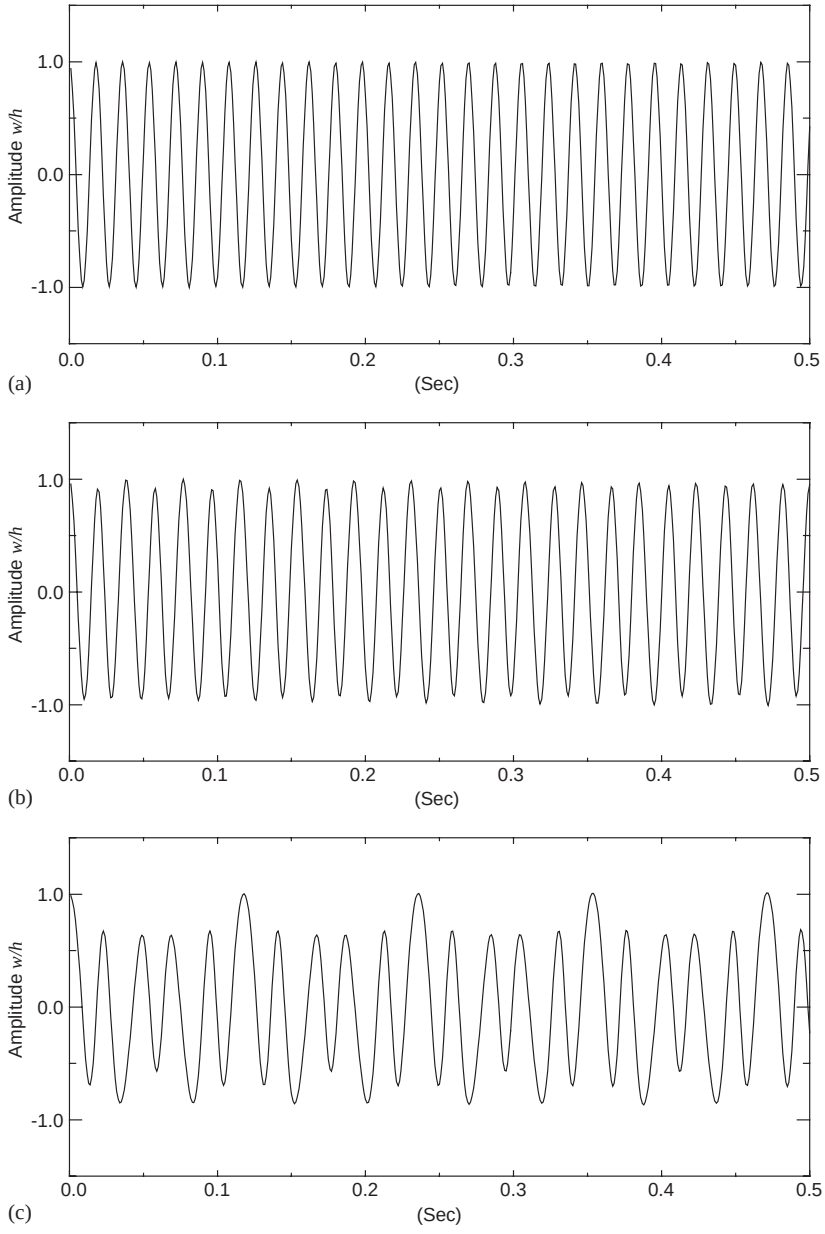

Fig. 5. The relationships between amplitude and time of the system ($k_1 = 0$, $\Delta T = 0$) corresponding to different magnetic field conditions: (a) $B_m = 0.1$ T (b) $B_m = 0.3$ T and (c) $B_m = 0.5$ T.

occurs in Fig. 7(b). Bolotin [21] indicated that the intensity of the beats decreases appreciably as the excitation frequency approaches the lower boundary of the unstable region. It can be seen in Fig. 7(a) for the lower boundary of the dynamic instability. For the resonance case, the amplitude of vibration becomes large and the damping cannot reduce the amplitude.

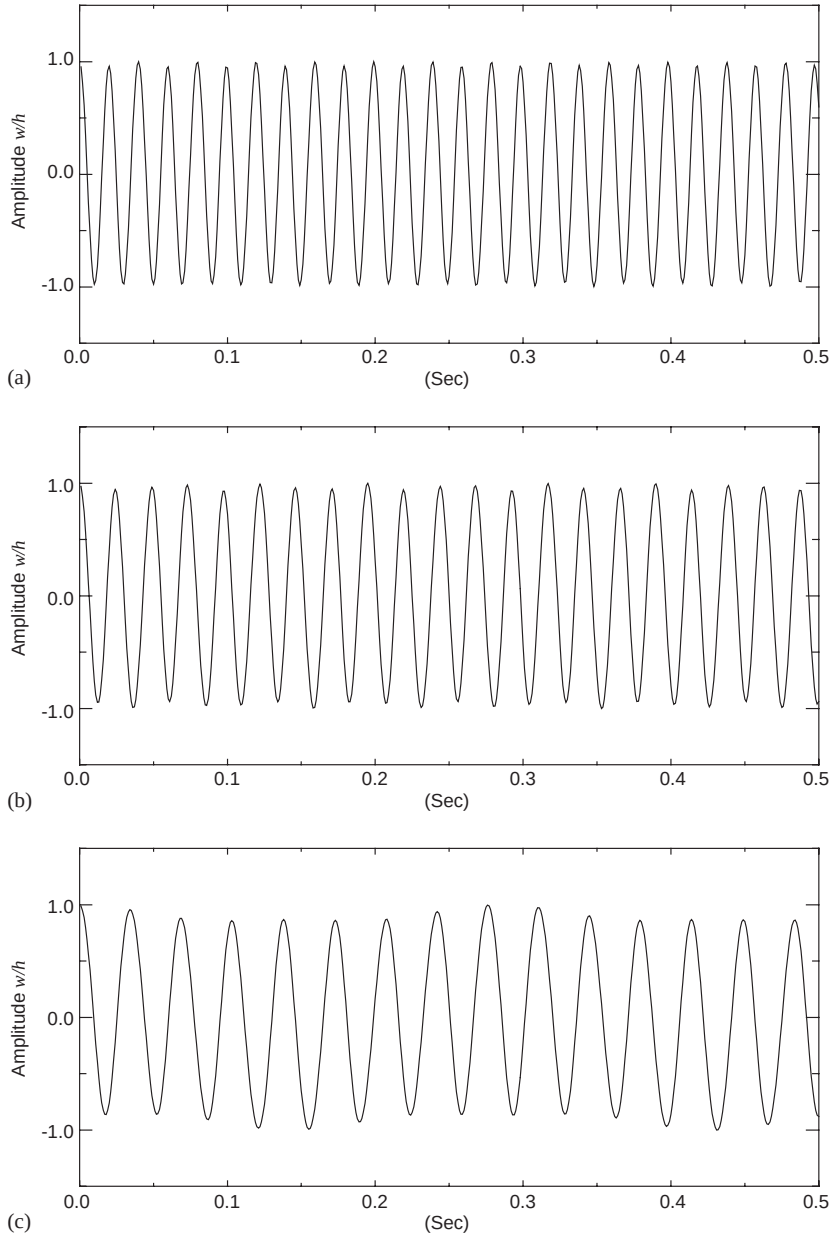

Fig. 6. The relationships between amplitude and time in a transverse magnetic field ($k_1 = 0$, $B_m = 0.2$ T) with different thermal loads: (a) $\Delta T = 1.0\,^{\circ}$C; (b) $\Delta T = 3.0\,^{\circ}$C; and (c) $\Delta T = 5.0\,^{\circ}$C.

For the same beam, k_1 is increased up to 0.0125, then the results are shown in Fig. 8. It should be noted that the previous beat phenomena in Figs. 7(a) and (c) become stable at this case because the damping is used, but the resonance still occurs in Fig. 8(c) when $\varpi = 258.2\,\mathrm{rad/s}$ is used. If the

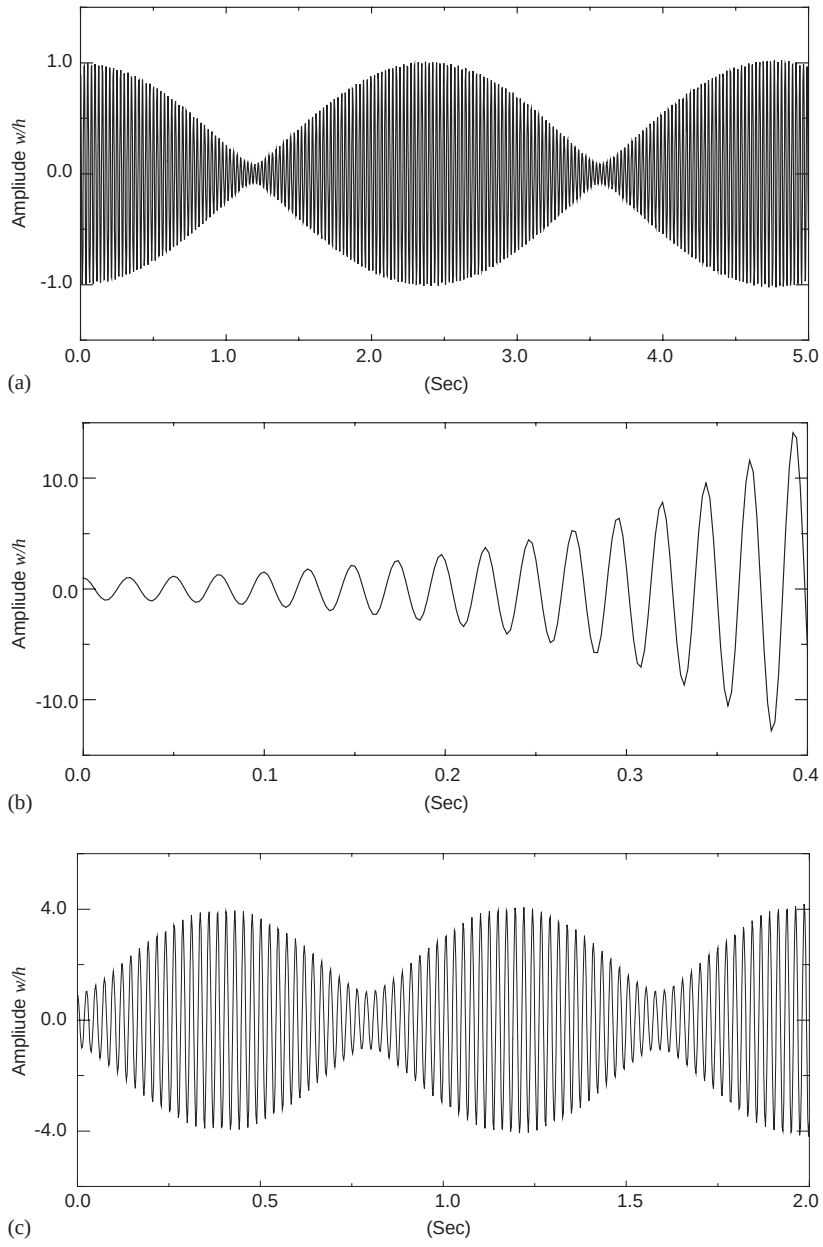

Fig. 7. The transient vibrations of the system ($k_1 = 0$, $B_m = 0.2$ T, and $\Delta T = 3.0\,^{\circ}$C) corresponding to different values of the excitation frequency ϖ are applied: (a) $\varpi = 250.5$ rad/s; (b) $\varpi = 258.2$ rad/s; and (c) $\varpi = 266.5$ rad/s.

excitation frequency $\varpi = 258.2$ rad/s is used as a constant, the damping parameter k_1 is increased and replaced by 0.026, 0.029, and 0.032, individually, then the results are shown in Fig. 9. The results show that the damping parameter $k_1 = 0.032$ is used for the stable case, $k_1 = 0.026$ is used

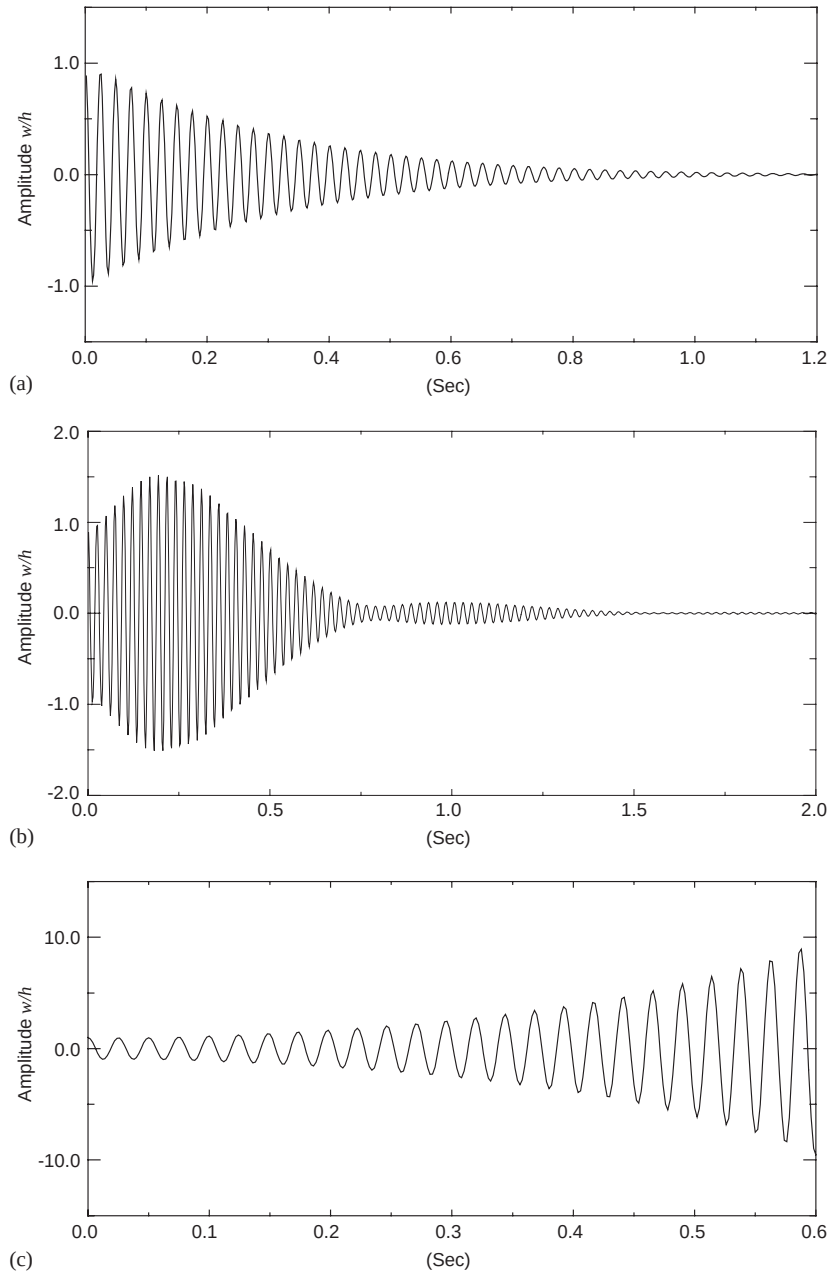

Fig. 8. The transient vibrations of the system ($k_1 = 0.0125$, $B_m = 0.2$ T, and $\Delta T = 3.0\,^{\circ}$C) corresponding to different values of the excitation frequency ϖ: (a) $\varpi = 250.5$ rad/s; (b) $\varpi = 266.5$ rad/s; and (c) $\varpi = 258.2$ rad/s.

for the resonance case, and $k_1 = 0.029$ is used for the critical case between the stable and unstable. The damping parameter $k_1 = 0.029$ is located on the boundary of the region of instability where the amplitude shows the steady-state motion nearly.

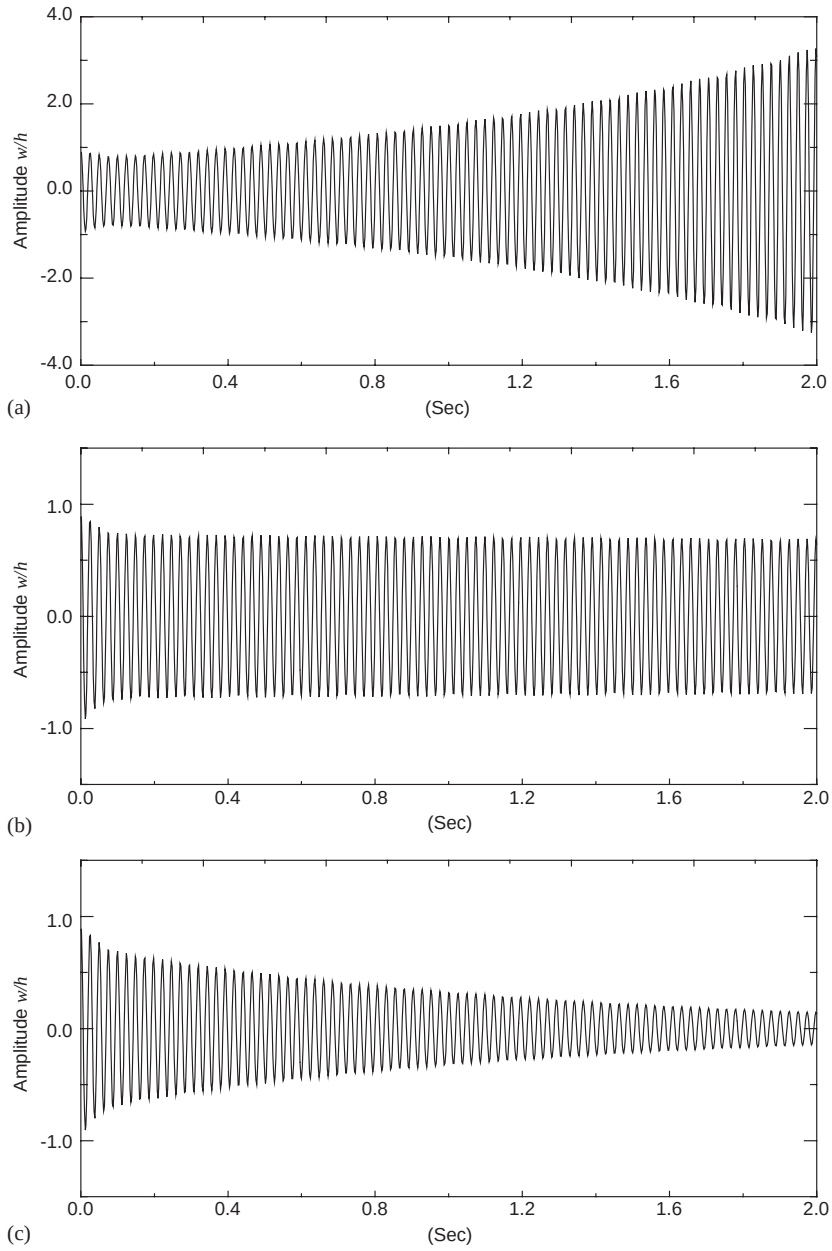

Fig. 9. The transient vibrations of the system ($B_m = 0.2$ T, $\Delta T = 3.0\,^{\circ}$C, and $\varpi = 258.2$ rad/s) corresponding to different values of damping parameter: (a) $k_1 = 0.026$; (b) $k_1 = 0.029$; and (c) $k_1 = 0.032$.

5. Conclusions

In this study, the magnetoelastic model of a pinned beam with the thermal loads is derived by means of Harmilton's principle, the assummed mode shape, and Galerkin's method. Using the

IHB method, a linearized incremental equation is obtained and the instability analysis is performed. In this small deflection analysis, the region of dynamic instability of a simply supported beam in an alternating magnetic field is very close to the results derived by Moon and Pao [3]. On the other hand, the transient vibratory behaviors are computed and discussed from the equation of motion by using the fourth-order Rung–Kutta method. The results of this study may be summarized as follows:

(1) Based on the assumption of the inextensible beam, the equation of motion in the transverse magnetic field leads to a nonlinear damping effect which is proportional to the square of amplitude. Also, the nonlinear damping effect is related to the conductivity of the material which is varied with temperature.
(2) Each buckling mode has its own safe temperature increase and magnetic field increase. Under the value of buckling, increasing either the transverse magnetic field or the thermal load leads to a decreasing fundamental natural frequency.
(3) Though the value of increased temperature is not high enough to produce buckling for slender sections in this study, the effect of thermal loads on the dynamic instability is obvious.
(4) While the different values of excitation frequency, ϖ, for the magnetic field are on the boundary of the region, in the region, and out of the region of dynamic instability, instability and steady vibrations are evident.

References

[1] S.A. Ambartsumian, Magneto-elasticity of thin plates and shells, *Applied Mechanics Reviews* 35 (1982) 1–5.
[2] F.C. Moon, Y.H. Pao, Magnetoelastic buckling of a thin plate, *Journal of Applied Mechanics* 35 (1968) 53–58.
[3] F.C. Moon, Y.H. Pao, Vibration and dynamic instability of a beam-plate in a transverse magnetic field, *Journal of Applied Mechanics* 36 (1969) 92–100.
[4] K. Miya, K. Hara, Y. Tabata, Experimental and theoretical study on magnetoelastic of a ferromagnetic cantilevered beam-plate, *Journal of Applied Mechanics* 45 (1978) 355–360.
[5] K. Miya, T. Takagi, Y. Ando, Finite element analysis of magnetoelastic buckling of a ferromagnetic beam-plate, *Journal of Applied Mechanics* 47 (1980) 377–382.
[6] A.C. Eringen, Theory of electromagnetic elastic plates, *International Journal of Engineering Science* 27 (1989) 363–375.
[7] J.S. Lee, Destabilizing effect of magnetic damping in plate strip, *Journal of Engineering Mechanics* 118 (1992) 161–173.
[8] Y.S. Shih, G.Y. Wu, J.S. Chen, Transient vibrations of a simply-supported beam with axial loads and transverse magnetic fields, *Mechanics of Structures and Machines* 26 (1998) 115–130.
[9] T. Tagaki, J. Tani, Y. Matsubara, T. Mogi, Dynamic behavior of fusion structural components under strong magnetic fields, *Fusion Engineering and Design* 27 (1995) 481–489.
[10] Y.H. Zhou, X.J. Zheng, A general expression of magnetic force for soft ferromagnetic plates in complex magnetic fields, *International Journal of Engineering Science* 35 (1997) 1405–1407.
[11] Y.H. Zhou, K. Miya, A theoretical prediction of natural frequency of a ferromagnetic beam-plate with low susceptibility in an in-plane magnetic field, *Journal of Applied Mechanics* 65 (1998) 121–126.
[12] Y.H. Zhou, Y.W. Gao, X.J. Zheng, Q. Jiang, Buckling and post-buckling of a ferromagnetic beam-plate induced by magnetoelastic interactions, *International Journal of Non-linear Mechanics* 35 (2000) 1059–1065.
[13] X.J. Zheng, X.Z. Wang, Analysis of magnetoelastic interaction of rectangular ferromagnetic plates with nonlinear magnetization, *International Solids and Structures* 38 (2001) 8641–8652.

[14] Q.S. Lu, C.W.S. To, K.L. Huang, Dynamic stability and bifurcation an alternating load and magnetic field excited magnetoelastic beam, *Journal of Sound and Vibration* 181 (1995) 873–891.
[15] S.L. Lau, Y.K. Cheung, Amplitude incremental variational principle for nonlinear vibration of elastic systems, *Journal of Applied Mechanics* 48 (1981) 959–964.
[16] S.L. Lau, Y.K. Cheung, S.Y. Wu, A variable parameter incrementation method for dynamic instability of linear and nonlinear systems, *Journal of Applied Mechanics* 49 (1982) 849–853.
[17] C. Pierre, E.H. Dowell, A study of dynamic instability of plates by an extended incremental harmonic balance method, *Journal of Applied Mechanics* 52 (1985) 693–697.
[18] S.L. Lau, S.W. Yuen, Solution diagram of non-linear dynamic systems by the IHB method, *Journal of Sound and Vibration* 167 (1993) 303–316.
[19] F. Ziegler, G. Rammerstorfer, Thermoelastic stability, in: R.B. Hetnarski (Ed.), *Thermal Stress*, Vol. III, Elsevier, Amsterdam, 1989.
[20] R.W.P. King, S. Prasad, *Fundamental Electromagnetic Theory and Applications*, Prentice-Hall, Englewood Cliffs, NJ, 1986.
[21] V.V. Bolotin, *The Dynamic Stability of Elastic Systems*, Holden-Day, San Francisco, 1964.